

Integrin-linked kinase as a target for ERG-mediated invasive properties in prostate cancer models

Daiiana D.Becker-Santos^{1,2,†}, Yubin Guo^{3,†},
Mazyar Ghaffari^{3,4}, Elaine D.Vickers³, Melanie Lehman³,
Manuel Altamirano-Dimas³, Arusha Oloumi¹,
Junya Furukawa³, Manju Sharma³, Yuzhuo Wang^{1,3,5},
Shoukat Dedhar^{1,2,3,6} and Michael E.Cox^{3,4,5,*}

¹Department of Integrative Oncology, British Columbia Cancer Research Centre, Vancouver, British Columbia, Canada V5Z 1L3, ²Genetics Graduate Program, University of British Columbia, Vancouver, Canada V6T 1Z2, ³The Vancouver Prostate Centre, Vancouver Coastal Health Research Institute, Vancouver, British Columbia, Canada V6H 3Z6, ⁴Experimental Medicine Program, Faculty of Medicine V5Z 1M9, ⁵Department of Urologic Sciences V5Z 1M9 and ⁶Department of Biochemistry and Molecular Biology, University of British Columbia, Vancouver, British Columbia, Canada V6T 1Z3

*To whom correspondence should be addressed. Tel: +604 875–4818;
Fax: +604 875–5654;
Email: mcox@prostatecentre.com

Approximately half of prostate cancers (PCa) carry *TMPRSS2-ERG* translocations; however, the clinical impact of this genomic alteration remains enigmatic. Expression of v-ets erythroblastosis virus E26 oncogene like (avian) gene (ERG) promotes prostatic epithelial dysplasia in transgenic mice and acquisition of epithelial-to-mesenchymal transition (EMT) characteristics in human prostatic epithelial cells (PrECs). To explore whether ERG-induced EMT in PrECs was associated with therapeutically targetable transformation characteristics, we established stable populations of BPH-1, PNT1B and RWPE-1 immortalized human PrEC lines that constitutively express flag-tagged ERG3 (fERG). All fERG-expressing populations exhibited characteristics of *in vitro* and *in vivo* transformation. Microarray analysis revealed >2000 commonly dysregulated genes in the fERG-PrEC lines. Functional analysis revealed evidence that fERG cells underwent EMT and acquired invasive characteristics. The fERG-induced EMT transcript signature was exemplified by suppressed expression of E-cadherin and keratins 5, 8, 14 and 18; elevated expression of N-cadherin, N-cadherin 2 and vimentin, and of the EMT transcriptional regulators Snail, Zeb1 and Zeb2, and lymphoid enhancer-binding factor-1 (LEF-1). In BPH-1 and RWPE-1-fERG cells, fERG expression is correlated with increased expression of integrin-linked kinase (ILK) and its downstream effectors Snail and LEF-1. Interfering RNA suppression of ERG decreased expression of ILK, Snail and LEF-1, whereas small interfering RNA suppression of ILK did not alter fERG expression. Interfering RNA suppression of ERG or ILK impaired fERG-PrEC Matrigel invasion. Treating fERG-BPH-1 cells with the small molecule ILK inhibitor, QLT-0267, resulted in dose-dependent suppression of Snail and LEF-1 expression, Matrigel invasion and reversion of anchorage-independent growth. These results suggest that ILK is a therapeutically targetable mediator of ERG-induced EMT and transformation in PCa.

Introduction

Identification of recurrent translocations in prostate cancer (PCa) involving androgen-responsive elements of transmembrane protease serine 2 gene,

Abbreviations: AR, androgen receptor; DMSO, dimethyl sulfoxide; EMT, epithelial-to-mesenchymal transition ERG, Expression of v-ets erythroblastosis virus E26 oncogene like (avian); ETS, E twenty-six; ILK, integrin-linked kinase; LEF-1, lymphoid enhancer-binding factor-1; PARP, poly (ADP ribose) polymerase; PCa, prostate cancer; PrECs, prostatic epithelial cells; PTEN, phosphatase and tensin homolog; siRNA, small interfering RNA.

[†]These authors contributed equally to this work.

TMPRSS2, and coding regions of E twenty-six (ETS) transcription factors (1) predict disease subtypes in which androgens could promote aberrant expression of these potential oncogenes (1–3). Fusions of *TMPRSS2* with *ERG* are the most common, presenting in approximately half of PCAs (4–6). *TMPRSS2* and *ERG* fusions can occur via reciprocal translocation or interstitial rearrangement, leading to aberrant androgen receptor (AR)-mediated expression of full-length or N-truncated ERG protein isoforms. Prior to identification of *TMPRSS2-ERG* translocations, ERG was recognized to be frequently expressed in PCa and to predict decreased disease-free survival (7). Although the prognostic value of *TMPRSS2-ERG* rearrangements in subsequent epidemiologic studies have been mixed, amplification of these translocations or linkage with loss of phosphatase and tensin homolog (PTEN) predicts poorer prognosis (8–15).

Aberrant expression of ETS factors, including ERG, has also been implicated in a range of malignancies, such as Ewing sarcoma, acute myeloid leukemia, primitive neuroectoderm tumors and cervical carcinomas, through regulation of an array of biological processes (16,17). With regard to PCa, *in vitro* and transgenic mouse studies demonstrate that expression of several *ERG* variants mediate transition to an invasive phenotype and transformation of immortalized prostatic epithelial models (14,18–22). Recent studies have begun to identify the molecular pathways by which ERG contributes to prostatic epithelial cell (PrEC) transformation. ERG expression suppresses prostatic epithelial differentiation (21) and promotes epithelial-to-mesenchymal transition (EMT) through FZD4-mediated WNT signaling and through activation of the ZEB1/ZEB2 axis in PCa cells (23,24). Acquisition of invasive characteristics by epithelial cells requires dramatic molecular changes, such as loss of cadherin-mediated cell–cell adhesion, remodeling of cell-matrix adhesion sites and basement membrane breakdown. These hallmarks of epithelial plasticity or EMT (25) are fundamental processes in embryonic development and metastatic progression of carcinomas (26).

Another factor shown to play a central role in EMT is integrin-linked kinase (ILK), an intracellular adaptor and serine/threonine kinase (27). ILK is involved in cytoskeletal dynamics and cell signaling cascades implicated in regulation of EMT, proliferation, survival, differentiation and angiogenesis. Importantly, ILK expression and activity are increased in a range of malignancies, including PCa, and inhibition of ILK is antitumorigenic. ILK can promote E-cadherin down-regulation by activating the transcriptional repressor Snail via poly (ADP ribose) polymerase-1 (PARP-1) in prostate and breast cancer cell lines (28). Additionally, over-expression of ILK results in down-regulation of epithelial markers cytokeratin 18 and MUC1, and up-regulation of mesenchymal markers lymphoid enhancer-binding factor-1 (LEF-1) and vimentin in several epithelial cell lines (29,30).

Here, we report that aberrant expression of ERG3 transforms three immortalized human PrECs, as measured by elevated, anchorage-independent growth *in vitro* and production of invasive renal capsule xenografts in NOD/SCID mice. ERG-transformed PrECs acquire morphologic and biochemical attributes of EMT, including suppressed expression of E-cadherin and cytokeratins 8/18 and elevated expression of N-cadherin and vimentin. ERG-expressing PrECs exhibit elevated expression of ILK and its effectors, Snail and LEF-1. Interfering RNA and small molecule inhibitor studies demonstrate ILK regulation of ERG-mediated PrEC transformation. These studies implicate ILK-mediated EMT as a therapeutically targetable ERG-regulated pathway involved in PCa progression.

Materials and methods

Cell culture

Human PrEC lines, PNT1B, courtesy Dr W.Jia (University of British Columbia), and BPH-1, courtesy Dr S.Hayward (Vanderbilt University), were maintained

in Dulbecco's modified Eagle's medium with 10% fetal bovine serum, whereas RWPE-1 (ATCC) was maintained in GIBCO™ Defined Keratinocyte-Serum-Free Media plus epidermal growth factor and bovine pituitary extract. All media and supplements were from Invitrogen (Burlington, Ontario, Canada). Mock- and flag-tagged ERG3 (fERG)-PrECs were created and characterized as detailed in [Supplementary Figure S1](#), available at [Carcinogenesis Online](#).

Protein analysis

Whole cell lysates were prepared in RIPA lysis buffer containing 2 mM Na₃VO₄, 1 mM NaF, 2 mM β-glycerolphosphate and complete protease inhibitor cocktail (Roche Diagnostics, Laval, Quebec, Canada). Immunoblots were performed with anti-ERG-1/2/3, anticytokeratin 8/18, anti-Oct1 (Santa Cruz Biotechnology, Santa Cruz, CA); anti-ILK, antivimentin, anti-E-cadherin and anti-N-cadherin (BD Biosciences, Mississauga, Ontario, Canada); anti-LEF-1, anti-Snail and anti-PARP (Cell Signaling, Danvers, MA); antimitogen-activated protein kinase (Millipore, Billerica, MA); anti-Flag and anti-β-actin (Sigma-Aldrich, Oakville, Ontario, Canada) and visualized using Alexa Fluor 680- (Invitrogen) and IRDye™ 800- (Cedarlane, Burlington, Ontario, Canada) conjugated antimouse or anti-rabbit IgG secondary antibodies with an Odyssey imaging system (Licor, Lincoln, NE). Densitometric analysis was performed using Gene Tools Ver. 4.0 software (SynGene, Cambridge, UK).

Messenger RNA analysis

Unless otherwise noted, molecular reagents were from Invitrogen or Qiagen (Mississauga, Ontario, Canada). Mock- and fERG-PrEC total cellular RNA was prepared using Trizol and complementary DNA cloned by reverse transcriptase-PCR using first-strand complementary DNA synthesis system. For ILK, Snail, E-cadherin and LEF-1 messenger RNA (mRNA), quantitative real-time PCR (qRT-PCR) was conducted using Roche Universal Probe Library technology (Roche Applied Science, Laval, Quebec, Canada) on an Applied Biosystems (Foster City, CA) qRT-PCR instrument with primers designed by the Roche Applied Science online assay design center. Relative transcript quantity was calculated using the ΔΔCt method of Applied Biosystems' analysis software. Results were normalized to β-actin mRNA levels and are reported as fold-change over the Mock values.

Microarray analysis Mock- and fERG-PrECs

For differential expression profiling of Mock- and fERG-PrECs, total RNA quality was assessed with the Agilent 2100 bioanalyzer prior to microarray analysis. Samples with a RIN value of ≥8.0 were prepared following Agilent's One-Color Microarray-Based Gene Expression Analysis Low Input Quick Amp Labeling v6.0. Total RNA (100 ng) was used to generate cyanine-3 labeled complementary RNA samples hybridized on Agilent Whole Human Genome Oligo Microarrays (Design ID 014850). Arrays were scanned with an Agilent DNA Microarray Scanner. Data were processed with Agilent Feature Extraction 10.5.1 and analyzed in Agilent GeneSpring 7.3.1. Data normalization involved flooring values <5.0 and median normalizing to the 50th percentile. To find significantly regulated genes, fold changes between the compared groups and *P*-values gained from *t*-test between same groups were calculated. The *t*-tests were performed on normalized data that had been log transformed, and the variances were not assumed to be equal between sample groups.

Anchorage-independent growth and anoikis assay

Anchorage-independent growth was assessed by soft agar colony formation of 5000 cells cultured for 10–14 days in 0.35% agar in respective culture media ± 10 μM of QLT-0267 or vehicle (dimethyl sulfoxide [DMSO]). Colonies were stained with 0.005% crystal violet, counted and measured microscopically. Anoikis was evaluated by culturing 5 × 10⁵ cells in polyhydroxyethyl-methacrylate- (polyHEMA; Sigma) coated plates in respective culture media ± 10 μM of QLT-0267 or vehicle for 48 h prior to lysis and immunoblotting for PARP cleavage.

Migration and invasion assays

The invasiveness of PrECs was evaluated using 8-μm-pore Matrigel Invasion Chambers (BD Biosciences). PrECs were transfected with small interfering RNAs (siRNAs) On-target plus SMART pool (Dharmacon) targeting human ERG (L-003886-00-0005), ILK (L-004499-00-0005) or non-targeting siRNA (Src: d-001810-01-05) for 2 days prior to seeding into transwells for invasion assays or harvest for immunoblotting. Alternatively, PrECs were treated with QLT-0267 (5 or 10 μM) or vehicle for 16 h before and during seeding into transwells for invasion assays. Equal numbers of the indicated cells were seeded in serum-free medium supplemented with 0.2% fatty-acid free bovine serum albumin into the upper chamber of the transwells. Epidermal growth factor and bovine pituitary extract were added to the lower chamber as a chemoattractant for RWPE-1 cells, and 20% fetal bovine serum was added to the lower chamber as a chemoattractant for BPH-1 cells. After 24 h, cells in the upper chamber were removed with a cotton swab and filters were washed twice

in phosphate-buffered saline. Cells present on the lower surface of the filters were fixed in methanol, stained with either crystal violet or 4',6-diamidino-2-phenylindole and photographed. Cells in six random fields were counted and averaged for each condition and the results of triplicate experiments were used to calculate mean ± standard error of the mean.

Three-dimensional (3-D) culture in Matrigel

Invasive characteristics were assessed by '3-D on-top culture' of cells in Matrigel (BD Biosciences). Single cell suspensions were cultured on Matrigel pre-coated 4-well chamber slides (Nalge Nunc, Rochester, NY) in standard media ± 5% Matrigel and 10 μM of QLT-0267 or vehicle for 5 days. This overlay medium was renewed every 2 days.

Renal capsule xenografts

Xenografts were prepared as described previously (31). Briefly, 2 × 10⁶ lineage-matched control and fERG-expressing PrECs were suspended in 50 μl neutralized type 1 rat tail collagen and grafted contralaterally under the renal capsule of 8–10-week-old male NOD/SCID mice (Charles River, Wilmington, MA) and palpated weekly for evidence of xenograft growth. At the indicated times, kidneys and grafts were excised from euthanized hosts, measured, formalin fixed and paraffin embedded for histology. Graft histology was scored by two independent pathologists from hematoxylin and eosin-stained and anti-ERG-1/2/3-stained 5-μm sections prepared from kidneys to include graft implantation sites. All animal procedures were performed according to the guidance of the Canadian Council on Animal Care and with protocol certification by the University of British Columbia Animal Care Committee.

Microscopy

Immunofluorescence analyses of 2-D and 3-D cultures were performed as described previously, respectively, (32,33) using the E-cadherin antibody, rhodamine-conjugated phalloidin and Hoechst DNA counter staining. Images were acquired with a Zeiss Axioplan 2 fluorescence microscope (Carl Zeiss Canada Ltd, Toronto, Canada), AxioCam HRc camera and AxioVision3.1 Software.

Statistical analysis

Analysis of ERG and E-cadherin expression in normal and metastatic PCA specimens was performed using a Kruskal–Wallis non-parametric analysis of variance and Dunn's multiple comparisons test. Cell growth and immunoblot data were analyzed from at least three independent biological replicates. Representative immunoblots and micrographs are provided to demonstrate the primary data. Differences in reporter activity, cell growth and tumor take rates were assessed by analysis of variance, Tukey's multiple comparisons test and paired *t*-tests. Anchorage-independent colony formation was assessed by χ² analysis. Immunoblot data were quantified by densitometry. Difference between xenograft growth kinetics was assessed by paired *t*-test of growth rates calculated by linear fit analysis.

Results

Expression of ERG in PrECs

In order to assess how aberrant expression of ERG might influence transformation and EMT in PrECs, we created stable blasticidin-resistant, Lenti viral fERG- and Mock-expression vector-infected populations from three immortalized, but non-tumorigenic human PrEC cell lines ([Supplementary Figure S1A](#), available at [Carcinogenesis Online](#)). PNT1B (34) and BPH-1 (35) are clonal SV40-immortalized normal adult PrEC lines reported to express large T antigen. RWPE-1 (36) is a clonal human papillomavirus-18 immortalized peripheral zone PrEC line derived from a histologically normal adult prostate. All three are reported to be cytokeratin-positive and to exhibit various attributes of apical PrECs.

ERG protein ([Figure 1A](#)) and mRNA ([Supplementary Figure S1B](#), available at [Carcinogenesis Online](#)) were readily detected in all three fERG populations. Sequential anti-Flag and anti-ERG immunoblotting of lysates from Mock- and fERG-PrECs detected identical bands of slightly larger than the 55 kD anti-ERG immunoreactive protein in HUVEC lysate, consistent with the predicted mass of fERG3. fERG protein was expressed in all three fERG-infected PrEC populations at levels 2- to 10-times that of ERG3 in HUVEC cells. Greater than 80% of the cells in each fERG-PrEC population expressed fERG by fluorescence-activated cell sorting analysis (data not shown). fERG exhibited a predominantly nuclear subcellular localization

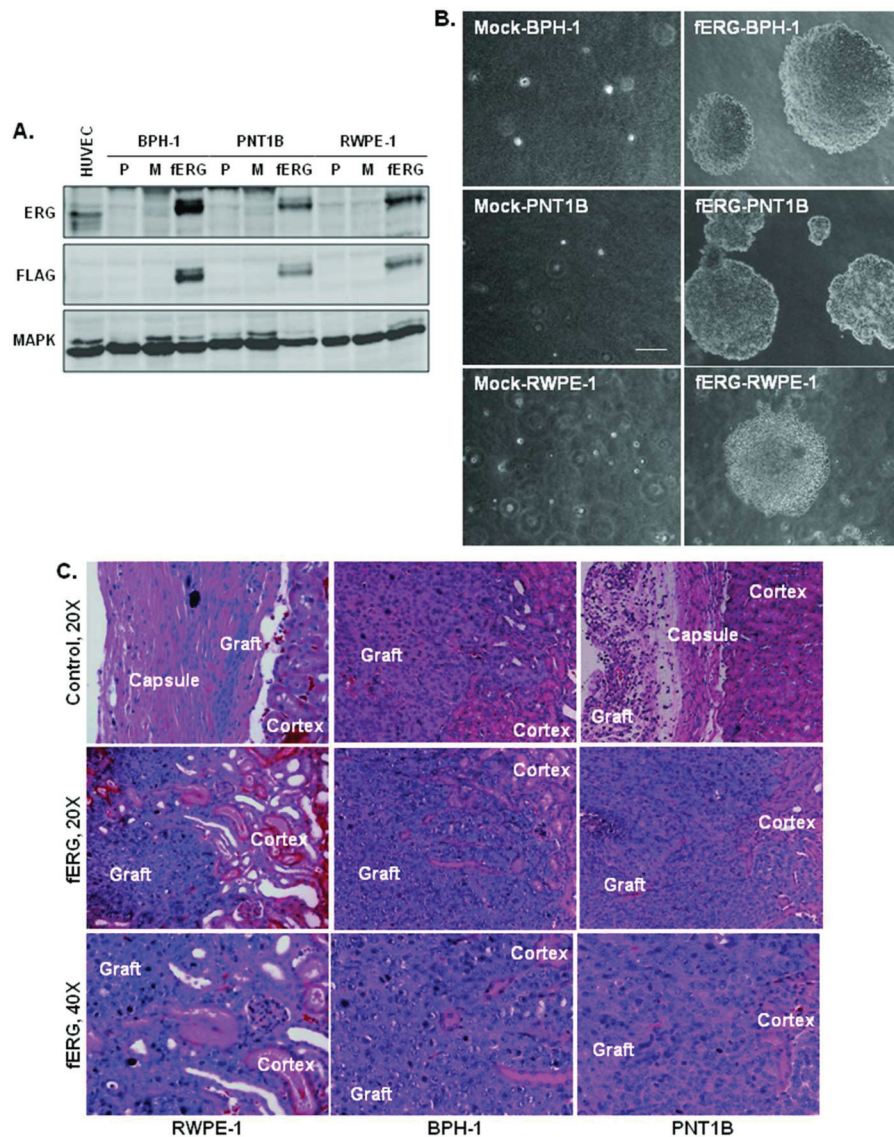


Fig. 1. Transformation of PrECs-expressing fERG. (A) Whole cell lysates of HUVEC, parental (P) and Mock (M)- and fERG-BPH-1, PNT1B and RWPE-1 cells were immunoblotted with anti-ERG (upper panel), anti-Flag (middle panel) and antimitogen-activated protein kinase (lower panel) antibodies. (B) Anchorage-independent growth was assessed by culturing each Mock- and fERG-PrEC population in soft agar for 10 days. Figure shows representative phase-contrast micrographs ($\times 10$) of soft agar colonies. Scale bar, 200 μm . (C). Representative hematoxylin and eosin micrographs (top and middle rows, $\times 20$; bottom row, $\times 40$) of control- (top row) and fERG-PrECs (middle and bottom rows) cells grafted onto contralateral renal capsules of NOD/SCID mice. BPH-1-grafted kidneys were harvested after 5 weeks, PNT1B-grafted kidneys after 6 weeks and RWPE-1-grafted kidneys after 8 weeks demonstrating morphologic differences in renal capsule growth, cortex invasion and cellular morphology. Quantification and statistical comparisons of soft agar colony formation and renal capsule xenograft growth are reported in [Supplementary Figure S2C](#), [S2D](#) and [S2E](#), available at [Carcinogenesis Online](#).

([Supplementary Figure S1C](#), available at [Carcinogenesis Online](#)) and was determined to be transcriptionally functional as assessed using an endoglin promoter-derived ETS-responsive reporter ([Supplementary Figure S1D](#), available at [Carcinogenesis Online](#)). All three fERG-expressing PrEC populations exhibited accelerated growth in tissue culture ([Supplementary Figure S2A](#) and [S2B](#), available at [Carcinogenesis Online](#)). These results established that the pDEST-fERG construct could direct appropriately localized and biologically active exogenous fERG expression in PrECs.

In vitro transformation of fERG-expressing PrECs

To determine if fERG expression impacted the phenotype of these PrEC models, we assessed anchorage-independent growth of fERG- and Mock-PrECs by soft agar colony formation ([Figure 1B](#); [Supplementary Figure S2C](#) and [S2D](#), available at [Carcinogenesis Online](#)). All three fERG-PrEC populations exhibited significantly

enhanced anchorage-independent growth compared with that of their respective Mock-PrEC populations. All fERG-expressing populations develop numerous, large colonies, whereas Mock-PNT1B and –RWPE-1 cells formed very few colonies >5 – 10 cell diameters. Mock-BPH-1 cells did form colonies at a rate, and of a size, that was distinguishable from zero by χ^2 test, revealing a subtle transformed phenotype. Nevertheless, these results indicate that the fERG-PrECs acquired *in vitro* transformed phenotype.

In vivo tumorigenesis of fERG-PrECs

We assessed whether the fERG-PrEC cells had acquired tumorigenic potential by grafting control and fERG-PrECs onto contralateral renal capsules of NOD/SCID mice ([Figure 1C](#)). All three fERG-PrEC xenografts showed 100% tumor formation. In all cases, the fERG-PrEC-grafted kidneys were completely overgrown by xenograft cells ([Supplementary Figure S3A](#), available at [Carcinogenesis Online](#)).

Relative xenograft growth rates of the fERG-expressing and control PrEC lines recapitulated *in vitro* soft agar colony formation results (Figure S2E). fERG-PrEC xenografts exhibited extremely neoplastic morphologies with extensive renal cortex invasion (Figure 1C). fERG xenografts could be identified by anti-ERG immunohistochemical staining, whereas Mock-PrEC grafts and adjacent renal cortex were not immunoreactive. (Supplementary Figure S3A, available at *Carcinogenesis* Online). Although histologically viable cells were detected in control cell grafts, these RWPE-1 and PNT1B grafts were no more than 6 mm³ when harvested. Control BPH-1 cells exhibited limited invasive xenograft growth; however, grafts were significantly

smaller (~one-fifth that of fERG-BPH-1 grafts). These results demonstrate that ERG expression is sufficient to transform these cell lines.

fERG expression dramatically alters transcript profile of PrECs

Transcriptional profiling was performed to compare differential expression in cognate Mock- and fERG-PrECs using Agilent G4112A Whole-Genome 60mer Oligo microarray chip kits. Analysis focused on data for 28 000 Stanford SOURCE annotated genes normalized from triplicate runs using the Bioconductor package, LIMMA. Setting a threshold of > or < 2-fold difference in expression, we found 2716 commonly dysregulated genes in all three cell lines; 60% up-regulated

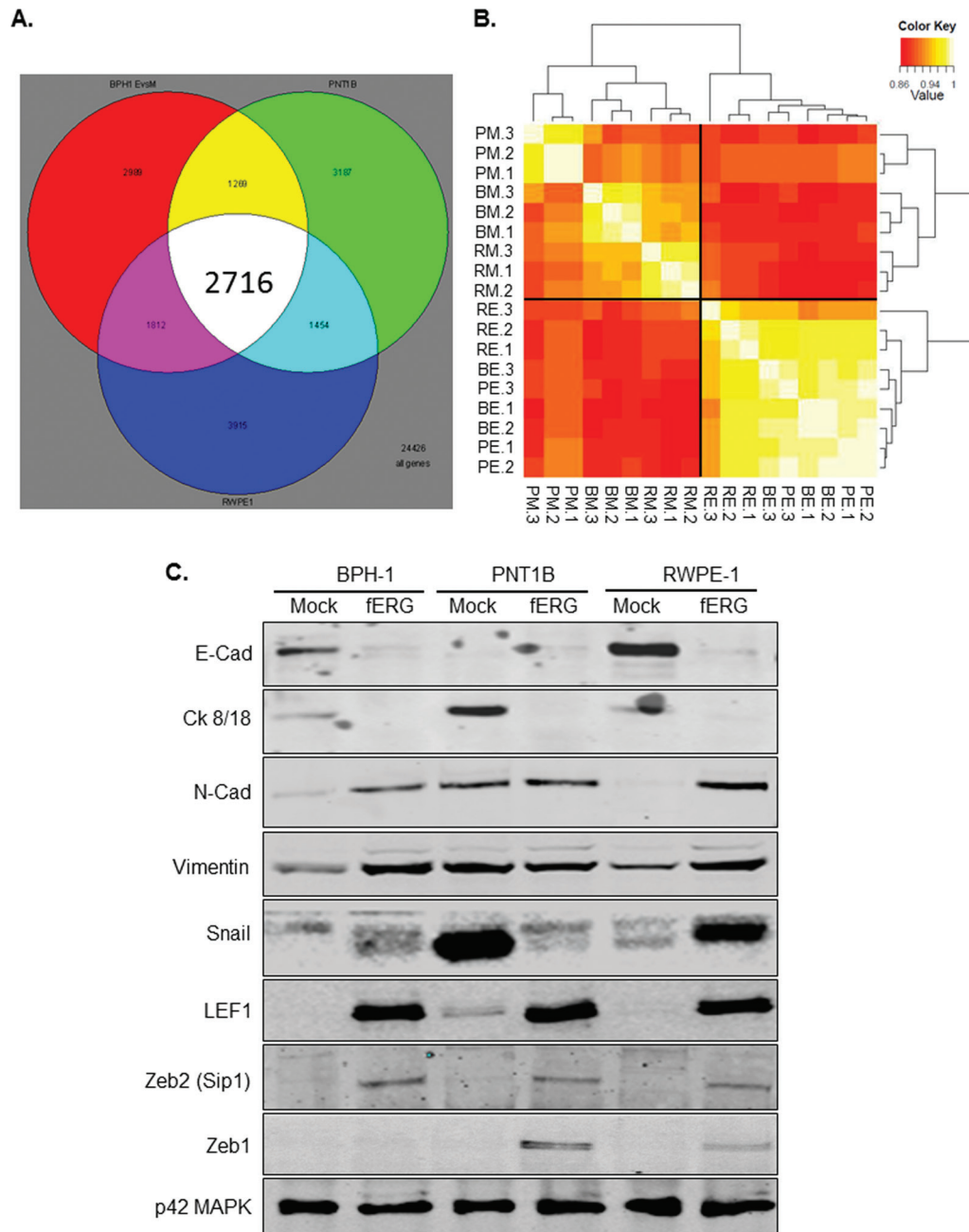


Fig. 2. EMT in PrECs-expressing fERG. Triplicate complementary DNA preparations were analyzed using Agilent's G4112A Whole-Genome 60mer Oligo Kit. (A) Focusing on Stanford SOURCE curate genes differentially expressed > or < 2-fold when comparing fERG:Mock (EvM) for RWPE-1 (R), BPH-1 (B) and PNT1B (P), 2716 were commonly dysregulated in all three cell lines. (B) Unsupervised hierarchical clustering segregates each Mock population and Mock-PrECs from fERG-PrECs but not the fERG-PrEC populations. (C) Whole cell lysates of HUVEC and Mock- and fERG-infected BPH-1, PNT1B and RWPE-1 cells were immunoblotted for expression of E-cadherin (E-Cad; upper panel), cytokeratin 8/18 (Ck 8/18; second panel), N-cadherin (N-Cad; middle panel) and vimentin (forth panel) versus MAP kinase (mitogen-activated protein kinase; bottom panel).

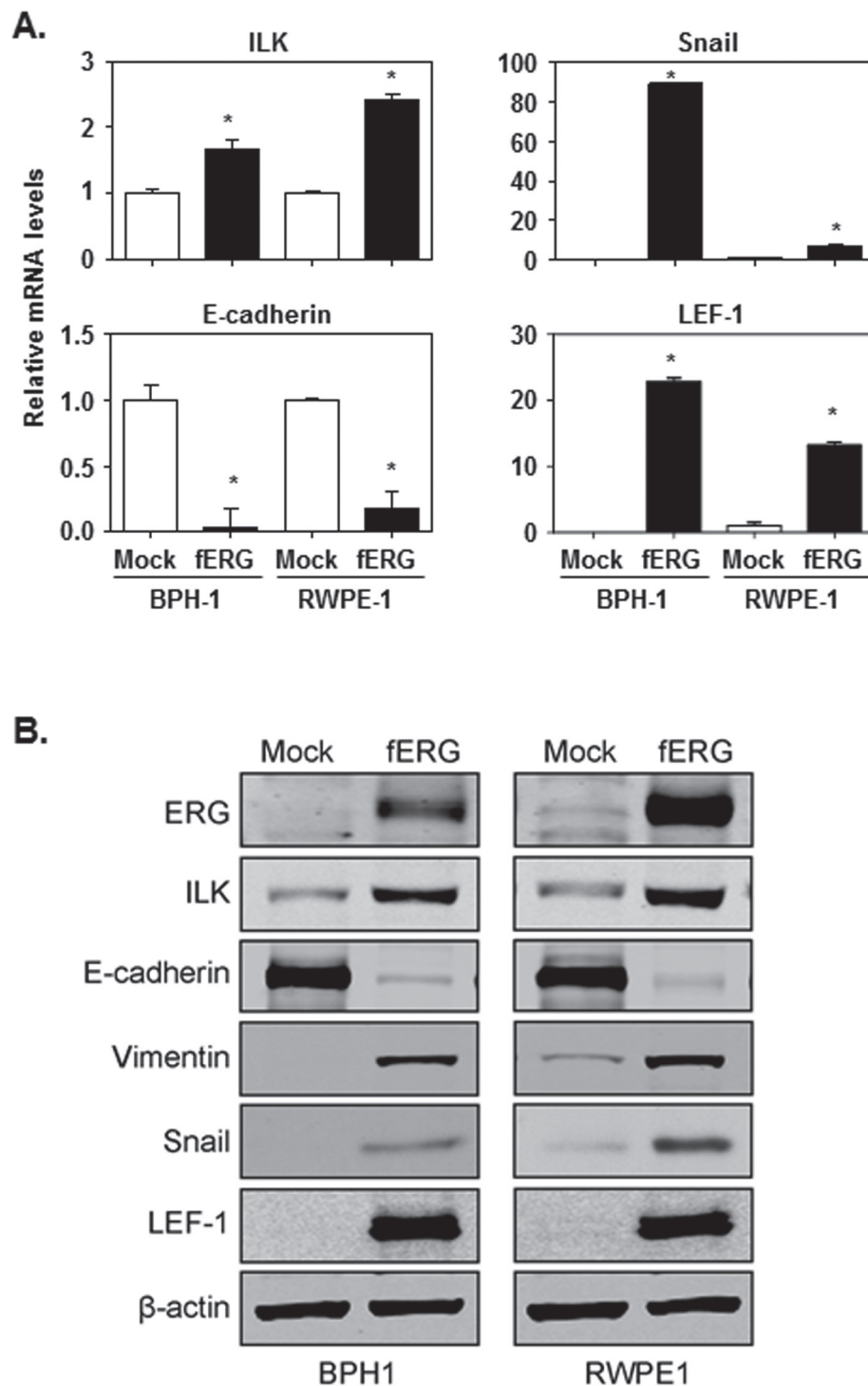


Fig. 3. Up-regulation of ILK and ILK-regulated proteins involved in EMT in fERG-PrECs. **(A)** qRT-PCR analysis of mRNA expression for ILK (upper left), E-cadherin (lower left), Snail (upper right) and LEF-1 (lower right) in Mock- (open bars) and fERG- (solid bars) BPH-1 and RWPE-1 cells. Ct values were normalized to β -actin mRNA levels reported as fold-change versus Mock cell values ($*P < 0.001$). **(B)** Whole cell lysate immunoblot analyses of ERG, ILK, E-cadherin, vimentin, Snail and LEF-1 protein levels in Mock- and fERG-BPH-1 and RWPE-1 cells using β -actin immunoblotting as a loading control.

and 40% down-regulated. Another ~4500 genes were found to be commonly dysregulated in two of the three cell lines (Figure 2A). Unsupervised hierarchical clustering segregates each Mock population and Mock-PrECs from fERG-PrECs but not the fERG-PrEC populations (Figure 2B).

Analysis of functional groupings for fERG/Mock-PrEC differential transcript profiles, using the Broad Institute Gene Set Enrichment Analysis tool (GSEA) of all differentially expressed genes, revealed

evidence for all three fERG-PrEC populations having undergone EMT and having acquired invasive characteristics (Supplementary Table S1, available at *Carcinogenesis* Online). The EMT transcript signature was exemplified by suppressed levels of the epithelial markers, E-cadherin and keratins 5, 8, 14 and 18; elevated levels of the mesenchymal markers, N-cadherin, N-cadherin2 and vimentin; and elevated levels of the EMT transcriptional regulators Snail, Zeb1 and Zeb2 and LEF-1 (Supplementary Table S2, available at *Carcinogenesis*

Online). These results are consistent with previous studies indicating that aberrant ERG expression induces EMT and transformation of PrECs (23,24).

fERG expression induces EMT in PrECs

The phenotypic changes observed in fERG-transformed PrECs are indicative of acquisition of mesenchymal characteristics associated with aggressive PCa (37). Given the recent report that ERG expression promotes EMT in PCa cells (23,24), and of Tables S1 and S2 indicating acquisition of EMT and invasive functional characteristics

in fERG-PrECs, we next validated expression of genes typically associated with EMT of PCa in Mock- and fERG-PrECs.

Expression of the prostatic luminal cell selective intermediate filament proteins, cytokeratins 8/18, was readily detected in Mock-PrECs and strongly suppressed in the fERG-PrECs. Additionally, in all three fERG-PrEC populations, and in Mock-PNT1B cells, E-cadherin protein expression was undetected or significantly suppressed (Figure 2C). Conversely, expression of the mesenchymal markers N-cadherin and vimentin was up-regulated in fERG-BPH-1 and -RWPE-1 cells relative to their cognate Mock populations.

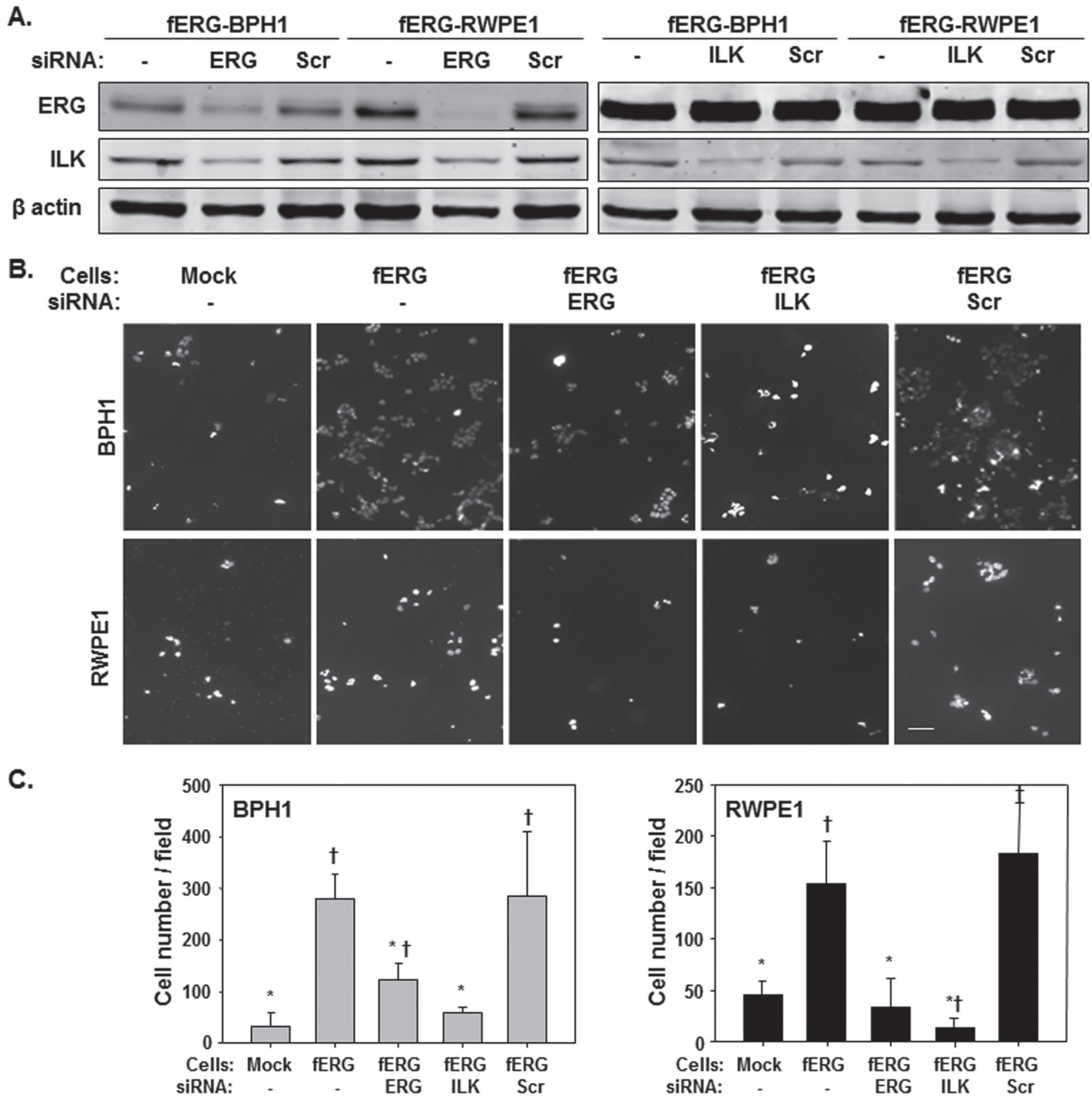


Fig. 4. Suppression of fERG or ILK expression disrupts Matrigel invasion of fERG-PrECs. (A) fERG-BPH-1 and -RWPE-1 cells were transfected with ERG- or ILK-targeted siRNA as described in Materials and methods for 2 days and lysates were immunoblotted for respective ILK and ERG expression using β -actin immunoblotting as a loading control. (B) Cells siRNA transfected as in A were plated onto Matrigel-coated transwell chambers and assayed for invasion after 1 day. Representative images of bottom of transwell chamber are provided, Scale bar, 100 μ m. (C) Quantification of invasion assays of respective Mock and fERG-PrECs expressed as average number of migrated cells per field in six random fields \pm standard error of the mean (*different than untreated fERG, $P < 0.01$, †different than Mock, $P < 0.01$).

Consistent with the loss of E-cadherin expression in the Mock-PNT1B cells, N-cadherin and vimentin expression was readily detected and indistinguishable in the Mock- and fERG-PNT1B populations indicating that the parental PNT1B cell line has already undergone partial EMT. Acquisition of mesenchymal characteristics of the fERG-PrECs was verified by immunohistochemical analysis of vimentin and E-cadherin expression in the renal capsule xenografts (Supplementary Figure S3C, available at *Carcinogenesis* Online). These results are consistent with induction of EMT in fERG-expressing PrECs and demonstrate that ERG expression profoundly alters the phenotype of immortalized PrECs to one consistent with that observed in aggressive PCa (23,38).

ILK, Snail and LEF-1 are up-regulated in fERG-PrECs

In order to investigate how fERG expression could mediate EMT in PrECs, we focused subsequent studies on BPH-1 and RWPE-1 cells because we observed high basal E-cadherin and cytokeratin expression in Mock cells that was strongly suppressed in fERG cells concomitant with increased N-cadherin and vimentin expression. As supporting evidence for EMT, in adherent culture, both fERG-PrEC lines exhibited acquisition of fusiform morphology concomitant with loss of cell-cell contact-associated E-cadherin expression, whereas Mock cells retained cobblestone morphology and cortical E-cadherin expression (Supplementary Figure S3D, available at *Carcinogenesis* Online).

LEF-1 and Snail mesenchymal transcriptional regulators are common molecular requirements in several models proposed to describe mechanisms of EMT induction under physiologic and pathologic conditions (26). Furthermore, ILK has been demonstrated to induce EMT in epithelial cells in a Snail and LEF-1-associated manner (39–41). We, therefore, examined the expression of ILK, Snail and LEF-1 in relation to that of E-cadherin, in Mock- and fERG-BPH-1 and -RWPE-1 cells. Both qRT-PCR and immunoblot techniques demonstrated that ILK, Snail and LEF-1 expression is increased in these fERG-PrECs (Figure 3A and 3B). When compared with the cognate Mock-PrEC populations, ILK expression in the fERG-PrECs is elevated ~2-fold and E-cadherin expression is suppressed by at least 80%, whereas Snail and LEF-1 expression are elevated at least 5-fold. Together with previous reports implicating expression of ILK, Snail and LEF-1 with PCa invasive potential (42–44), these results suggest that ERG may be a regulator of these features in *TPRSS2-ERG* fusion-positive PCa.

Suppression of fERG or ILK expression disrupts Matrigel invasion of fERG-PrECs

To assess whether ERG and ILK expression was linked to invasive potential of fERG-PrECs, we performed Matrigel invasion assays on fERG-BPH-1 and -RWPE-1 cells after siRNA silencing of ERG or ILK expression (Figure 4). Treating both cell lines with an ERG-targeted siRNA resulted in substantially suppressed ERG and ILK expression, whereas treatment with an ILK-targeted siRNA resulted in suppressed ILK expression without affecting ERG expression (Figure 4A). This suggests that ERG expression is upstream of ILK.

To determine how suppression of ERG or ILK impacted invasive potential of fERG-PrECs, invasion across Matrigel-coated transwells of control and siRNA-treated cells was compared with that of the respective Mock-PrECs (Figure 4B and 4C). Consistent with the invasive characteristics of fERG-PrECs in renal capsule xenografts, fERG-BPH-1 cells invaded 8.7 times more than Mock-BPH-1 cells and fERG-RWPE-1 cells invaded 3.4 times more than Mock-RWPE-1 cells. Suppression of ERG or ILK expression significantly suppressed Matrigel invasion of both fERG-PrECs. The invasion rate of ERG siRNA-treated fERG-BPH-1 and -RWPE-1 cells were 44% and 22% of respective untreated fERG-PrECs. Similarly, the invasion rate of ILK siRNA-treated fERG-BPH-1 and -RWPE-1 cells were 21% and 9% of respective untreated fERG-PrECs. Invasion rates of respective ERG and ILK siRNA-treated fERG-PrECs were indistinguishable from each other indicating that suppression of either target reversed the acquired invasive potential of the cell lines.

Inhibition of ILK activity decreases Snail and LEF-1 expression, impairs *in vitro* invasive properties and inhibits anchorage-independent growth of fERG-BPH-1 cells

ILK has been shown to up-regulate expression of LEF-1 (30,39) and Snail (28,39) and the ILK-selective small molecule kinase inhibitor, QLT-0267, has been shown to block ILK-induced expression of these EMT regulators (45,46). Similarly, treating fERG-BPH-1 cells with QLT-0267 resulted in a dose-dependent decrease in Snail and LEF-1 protein expression (Figure 5A). These results implicate ILK expression and activity in ERG-mediated EMT by up-regulating expression of Snail and LEF-1 protein levels.

The role of ILK in regulating invasive migratory capacity of fERG-BPH-1 cells was assessed using Matrigel-coated transwell assays (Figure 5B). Matrigel invasion of fERG cells was approximately 2-fold greater than the cognate mock cells. Treatment of fERG-PrECs with 5 and 10 μ M of QLT-0267 resulted in a dose-dependent inhibition of transwell invasion such that the invasive capacity of fERG-BPH-1 cells treated with 5 μ M QLT-0267 was indistinguishable from that of Mock-BPH-1 cells; whereas 10 μ M of QLT-0267 suppressed Matrigel invasion to levels significantly less than that observed in Mock-BPH-1 cells.

The impact of QLT-0267 on fERG-BPH-1 growth was further assessed using a 3-D culture of BPH-1 cells on Matrigel. In these assays, Mock-BPH-1 cells formed well-defined epithelial spheroid structures, with organized cortical F-actin cytoskeleton and E-cadherin expression,

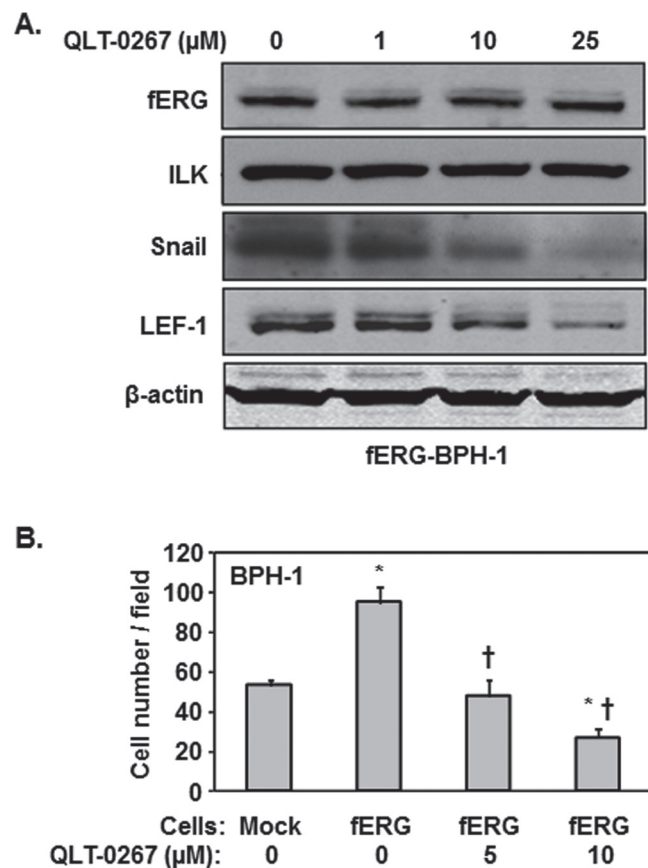


Fig. 5. QLT-0267 treatment decreases LEF-1 and Snail expression and impairs *in vitro* invasive properties of fERG-BPH-1 cells. (A) Immunoblot analysis of fERG-BPH-1 cells after 48 h treatment with DMSO (0) or the indicated doses of QLT-0267 for expression of ERG, ILK, Snail and LEF-1 using β -actin immunoblotting as a loading control. (B) Quantification of Matrigel invasion assay of cells treated as in A for 24 h expressed as average number of migrated cells per field in 6 random fields \pm standard error of the mean (* different than Mock, $P < 0.01$, † different than untreated fERG, $P < 0.01$).

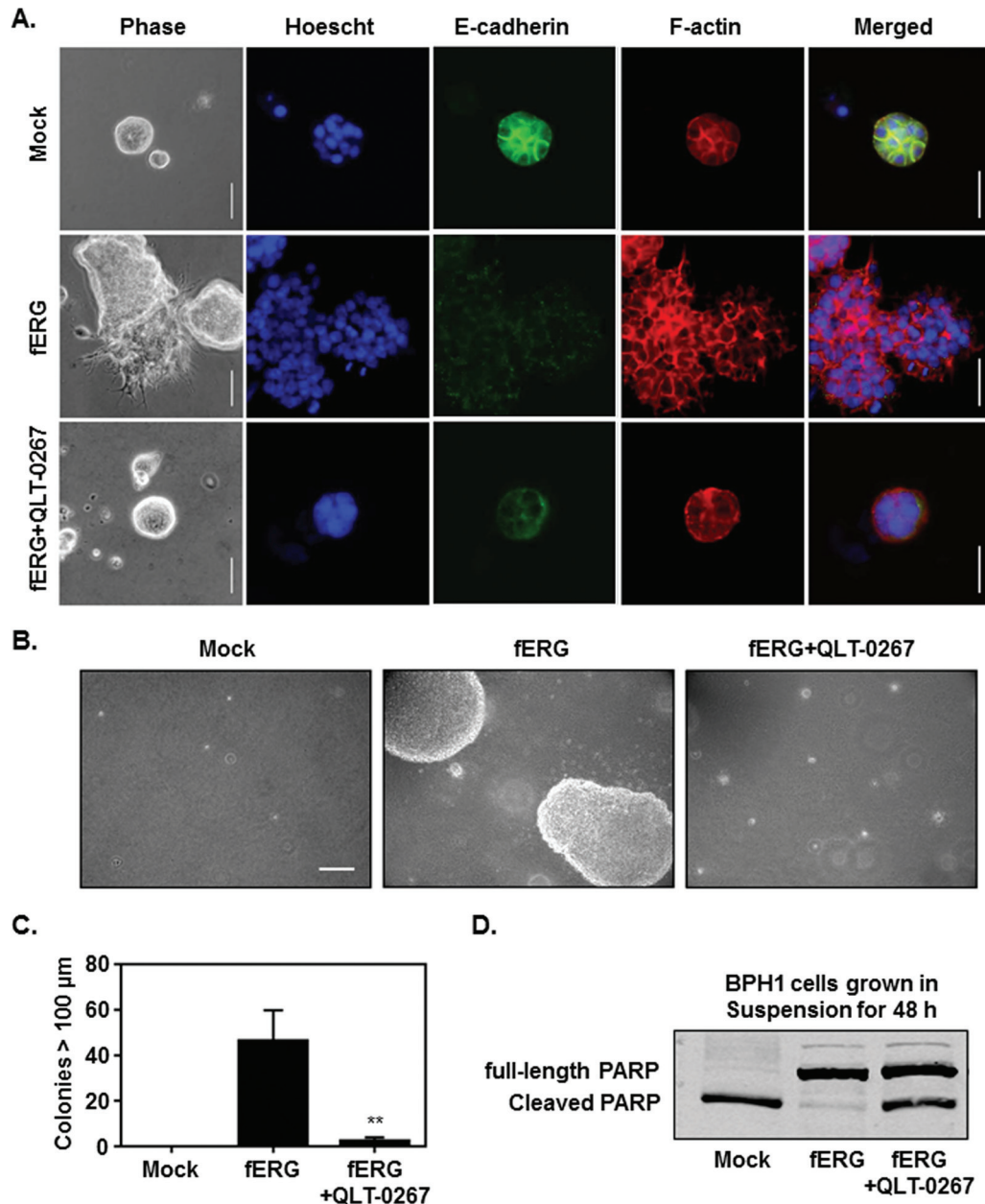


Fig. 6. QLT-0267 treatment reverts transformed phenotype of fERG-BPH-1 cells. **(A)** Phase-contrast images (left column) of 3-D cultures in Matrigel of Mock-BPH-1 and DMSO or QLT-0267-treated fERG-BPH-1 cells as described in Materials and Methods. Immunofluorescence staining of chromatin (Hoescht), E-cadherin, F-actin and merged fluorescence images of the same field (2–5 columns, as indicated). Scale bar, 50 μm. **(B)** Representative phase-contrast micrographs of soft agar colonies of Mock-BPH-1 in standard media (right panel), and BPH-1-fERG cells in DMSO (middle panel) or 10 μM QLT-0267 (right panel) cultured for 14 days. Scale bar, 200 μm. **(C)** Histogram shows mean number of colonies/well >100 μm ± standard deviation ($P < 0.005$). **(D)** PARP immunoblot analysis of lysates from Mock-BPH-1 cells cultured in standard media (left lane) and fERG-BPH-1 cells cultured in DMSO (middle lane) or 10 μM QLT-0267 (right panel) on polyHEMA-coated plates for 48 h. Uncleaved full-length PARP is indicated as the upper (116 kDa) band and caspase-cleaved PARP is indicated by the lower (89 kDa) band.

consistent with features of differentiated, non-transformed PrECs (Figure 6A). In contrast, fERG-BPH-1 cells formed large irregular cellular aggregates with dramatically suppressed E-cadherin expression and disorganized F-actin cytoskeleton with extensions radiating from the aggregates indicative of invasive behavior. Treatment of fERG-BPH-1 cells with QLT-0267 inhibited formation of these disorganized aggregates and resulted in formation of compact spheroid structures resembling structures formed by Mock-BPH-1 cells and partial restoration of E-cadherin expression, consistent with a reversion of the EMT phenotype.

Because ILK has been shown previously to induce resistance to anoikis and anchorage-independent growth of epithelial cells (47,48),

we examined how ILK impacts anchorage-independent growth of fERG-BPH-1 cells. Relative to Mock-BPH-1 cells, fERG-BPH-1 cells formed numerous large colonies when cultured in soft agar; however, colony growth was strongly suppressed (~10-fold) when treated with QLT-0267 (Figure 6B and 6C). In order to evaluate whether targeting ILK restored induction of apoptosis due to the loss of substrate adhesion, that is anoikis (49), PARP cleavage was assessed in BPH-1 cells cultured in suspension (Figure 6D). Mock cells in suspension readily underwent apoptosis, as evidenced by the almost exclusive detection of cleaved PARP. In contrast, PARP was predominantly detected in its intact form in fERG-BPH-1 cells cultured in suspension consistent with them being resistant to anoikis. However, treatment of suspension

cultures of fERG-BPH-1 cells with QLT-0267 partially restored sensitivity to anoikis as assessed by induction of cleavage of approximately 40% of total PARP. These results implicate ILK in regulating anchorage-independence and strongly implicate ILK as an ERG-induced mediator of PCa carcinogenesis.

Discussion

Although ERG is appreciated to promote transformation of prostatic epithelium (14,19–22) and to promote EMT (23), the underlying mechanism(s) and therapeutic potential remain to be fully elucidated. Consistent with its role in Ewing's, acute myeloid leukemia and neuroectoderm oncogenesis, ERG fusions are probably to play a role in prostate tumorigenesis through transcriptional induction or repression of downstream targets. Data presented here provide evidence supporting observations linking ERG expression to transformation and EMT in a panel of PrECs and is the first to demonstrate that acquisition of these transformed properties is at least partially controlled by ILK. Our results suggest a model in which aberrant ERG expression promotes up-regulated ILK expression and activation that drives EMT and promotes PrEC transformation via up-regulation of Snail and LEF-1. The resulting suppression of cytokeratin 8/18 and E-cadherin, as well as expression of N-cadherin and vimentin, are hallmarks of an EMT transcript profile change that allows tumor cells to overcome contact inhibition and enhance metastatic potential (37).

Aggressive PCa has been associated with acquisition of mesenchymal characteristics (37). Highlighting our findings that the ILK-associated mesenchymal markers, Snail and LEF-1, are up-regulated in ERG-expressing cells are studies implicating Snail and LEF-1 in prostate tumorigenesis and invasion. Snail expression is noted to be increased in PCa cells exhibiting invasive properties (43), whereas LEF-1 is highly expressed in androgen-independent PCa (44). Our demonstration that ILK inhibition leads to down-regulation of ERG-mediated LEF-1 and Snail expression, partial restoration of E-cadherin expression and suppression of invasive and anchorage-independent growth properties mechanistically link ERG expression to ILK-mediated PrEC transformation.

Our observation that ERG-driven ILK expression can lead to anchorage-independent growth and increased invasive potential are intriguing in light of previous evidence that ILK expression is associated with aggressive PCa phenotypes and correlated with poor prognosis (42). Furthermore, our demonstration that these processes can occur in AR-negative (BPH-1 and PNT1B) and AR-low (RWPE-1) PrEC model cell lines are consistent with previously proposed models for ERG acting to antagonizing normal PrEC differentiation by suppressing AR expression and signaling (21,50) and support conclusions in the emerging literature indicating that ERG fusions are associated with a more aggressive disease (4,8,10,12,51–53).

Two of the PrEC lines used here (PNT1B and RWPE-1) have been reported to exhibit increased *in vitro* invasive and mitotic properties; however, reports of them being transformed by aberrant ETS gene expression have been variable (2,14,18–23). The reasons underlying this difference in outcome are probably due to some combination of differences in epitope tagging, viral infection and/or promoter activity. However, our observation that fERG-PrECs developed highly mitotic, invasive tumors is consistent with reports of increased metastatic and mitotic properties of ETS-expressing PrECs. Furthermore, although the three PrEC lines modeled here exhibit variable prostatic epithelial characteristics, fERG-expressing cells uniformly exhibit mesenchymal molecular and morphologic features. These results suggest that ERG expression is capable of inducing a similar oncogenic program in cells with variable intrinsic apical cell characteristics.

Our results suggest that in ERG-expressing PCas, ILK-regulated proteins are effectors of EMT and suggest the possibility that ILK may serve as a therapeutic target in ERG-expressing PCas. This conclusion is supported by the observation that ILK promotes EMT and associated drug resistance in hepatocellular carcinoma and that ILK inhibition increases sensitivity of these cells to epidermal growth factor receptor-targeted therapies (54). Further support for ILK as a promising

therapeutic target in PCa comes from recent reports demonstrating that *TMPRSS2-ERG* gene fusions and PTEN loss cooperatively promote PCa progression (13,14,55). ILK inhibition suppresses AKT activation and induces apoptosis in PTEN-deficient PCa cells (56) and delays growth of PTEN-negative tumors (57). Thus, targeting ILK in PCa may be very promising because it might potentially affect ERG and PTEN aberrant signaling, which together seem to be pivotal in prostate carcinogenesis. Demonstration that aberrant ERG expression is capable of promoting EMT and transformation of these immortalized PrECs provides models for determining if, or what, predilections are essential for oncogenic susceptibility to ETS-mediated PCa etiology, to guide subsequent efforts to identify common molecular and phenotypic responses to ERG expression, and to validate and therapeutically target these markers.

Supplementary material

Supplementary Tables S1 and S2 and Figures S1–S3 can be found at <http://carcin.oxfordjournals.org/>

Funding

Cancer Research Society, Inc. and Canadian Institute for Health Research to M.E.C; National Cancer Institute of Canada with funds from the Terry Fox Foundation to S.D. and M.E.C; and National Institute of Health Pacific Northwest Prostate Cancer SPORE (P50CA097186 to B.K. and P.N.).

Acknowledgements

We thank Yuwei Wang (British Columbia Cancer Agency) for animal model technical support and Quadra Logic Technology Inc (QLT Inc), Vancouver, British Columbia for supplying QLT-0267.

Conflict of Interest Statement: S.D. is a scientific consultant for Quadra Logic Technology Inc. (QLT Inc), Vancouver.

References

- Tomlins, S.A. *et al.* (2005) Recurrent fusion of *TMPRSS2* and ETS transcription factor genes in prostate cancer. *Science*, **310**, 644–648.
- Helgeson, B.E. *et al.* (2008) Characterization of *TMPRSS2:ETV5* and *SLC45A3:ETV5* gene fusions in prostate cancer. *Cancer Res.*, **68**, 73–80.
- Mehra, R. *et al.* (2007) Heterogeneity of *TMPRSS2* gene rearrangements in multifocal prostate adenocarcinoma: molecular evidence for an independent group of diseases. *Cancer Res.*, **67**, 7991–7995.
- Perner, S. *et al.* (2006) *TMPRSS2:ERG* fusion-associated deletions provide insight into the heterogeneity of prostate cancer. *Cancer Res.*, **66**, 8337–8341.
- Kumar-Sinha, C. *et al.* (2008) Recurrent gene fusions in prostate cancer. *Nat. Rev. Cancer*, **8**, 497–511.
- Tomlins, S.A. *et al.* (2009) ETS gene fusions in prostate cancer: from discovery to daily clinical practice. *Eur. Urol.*, **56**, 275–286.
- Petrovics, G. *et al.* (2005) Frequent overexpression of ETS-related gene-1 (*ERG1*) in prostate cancer transcriptome. *Oncogene*, **24**, 3847–3852.
- Rajput, A.B. *et al.* (2007) Frequency of the *TMPRSS2:ERG* gene fusion is increased in moderate to poorly differentiated prostate cancers. *J. Clin. Pathol.*, **60**, 1238–1243.
- Barry, M. *et al.* (2007) *TMPRSS2-ERG* fusion heterogeneity in multifocal prostate cancer: clinical and biologic implications. *Urology*, **70**, 630–633.
- Nam, R.K. *et al.* (2007) Expression of *TMPRSS2:ERG* gene fusion in prostate cancer cells is an important prognostic factor for cancer progression. *J. Urol.*, **177**, 467–468.
- FitzGerald, L.M. *et al.* (2008) Association of *TMPRSS2-ERG* gene fusion with clinical characteristics and outcomes: results from a population-based study of prostate cancer. *BMC Cancer*, **8**, 230.
- Attard, G. *et al.*; Transatlantic Prostate Group. (2008) Duplication of the fusion of *TMPRSS2* to *ERG* sequences identifies fatal human prostate cancer. *Oncogene*, **27**, 253–263.
- Yoshimoto, M. *et al.* (2008) Absence of *TMPRSS2:ERG* fusions and PTEN losses in prostate cancer is associated with a favorable outcome. *Mod. Pathol.*, **21**, 1451–1460.
- Carver, B.S. *et al.* (2009) Aberrant ERG expression cooperates with loss of PTEN to promote cancer progression in the prostate. *Nat. Genet.*, **41**, 619–624.

15. Markert, E.K. *et al.* (2011) Molecular classification of prostate cancer using curated expression signatures. *Proc. Natl. Acad. Sci. U.S.A.*, **108**, 21276–21281.
16. Seth, A. *et al.* (2005) ETS transcription factors and their emerging roles in human cancer. *Eur. J. Cancer*, **41**, 2462–2478.
17. Turner, D.P. *et al.* (2008) ETS transcription factors: oncogenes and tumor suppressor genes as therapeutic targets for prostate cancer. *Expert Rev. Anticancer Ther.*, **8**, 33–42.
18. Tomlins, S.A. *et al.* (2008) Role of the TMPRSS2-ERG gene fusion in prostate cancer. *Neoplasia*, **10**, 177–188.
19. Klezovitch, O. *et al.* (2008) A causal role for ERG in neoplastic transformation of prostate epithelium. *Proc. Natl. Acad. Sci. U.S.A.*, **105**, 2105–2110.
20. Hollenhorst, P.C. *et al.* (2004) Expression profiles frame the promoter specificity dilemma of the ETS family of transcription factors. *Nucleic Acids Res.*, **32**, 5693–5702.
21. Sun, C. *et al.* (2008) TMPRSS2-ERG fusion, a common genomic alteration in prostate cancer activates C-MYC and abrogates prostate epithelial differentiation. *Oncogene*, **27**, 5348–5353.
22. Hu, Y. *et al.* (2008) Delineation of TMPRSS2-ERG splice variants in prostate cancer. *Clin. Cancer Res.*, **14**, 4719–4725.
23. Gupta, S. *et al.* (2010) FZD4 as a mediator of ERG oncogene-induced WNT signaling and epithelial-to-mesenchymal transition in human prostate cancer cells. *Cancer Res.*, **70**, 6735–6745.
24. Leshem, O. *et al.* (2011) TMPRSS2/ERG promotes epithelial to mesenchymal transition through the ZEB1/ZEB2 axis in a prostate cancer model. *PLoS ONE*, **6**, e21650.
25. Savagner, P. (2001) Leaving the neighborhood: molecular mechanisms involved during epithelial-mesenchymal transition. *Bioessays*, **23**, 912–923.
26. Kalluri, R. *et al.* (2009) The basics of epithelial-mesenchymal transition. *J. Clin. Invest.*, **119**, 1420–1428.
27. McDonald, P.C. *et al.* (2008) Integrin-linked kinase—essential roles in physiology and cancer biology. *J. Cell. Sci.*, **121**(Pt 19), 3121–3132.
28. McPhee, T.R. *et al.* (2008) Integrin-linked kinase regulates E-cadherin expression through PARP-1. *Dev. Dyn.*, **237**, 2737–2747.
29. Guaita, S. *et al.* (2002) Snail induction of epithelial to mesenchymal transition in tumor cells is accompanied by MUC1 repression and ZEB1 expression. *J. Biol. Chem.*, **277**, 39209–39216.
30. Novak, A. *et al.* (1998) Cell adhesion and the integrin-linked kinase regulate the LEF-1 and beta-catenin signaling pathways. *Proc. Natl. Acad. Sci. U.S.A.*, **95**, 4374–4379.
31. Wang, Y. *et al.* (2001) A human prostatic epithelial model of hormonal carcinogenesis. *Cancer Res.*, **61**, 6064–6072.
32. Fielding, A.B. *et al.* (2008) Integrin-linked kinase localizes to the centrosome and regulates mitotic spindle organization. *J. Cell Biol.*, **180**, 681–689.
33. Lee, G.Y. *et al.* (2007) Three-dimensional culture models of normal and malignant breast epithelial cells. *Nat. Methods*, **4**, 359–365.
34. Cussenot, O. *et al.* (1991) Immortalization of human adult normal prostatic epithelial cells by liposomes containing large T-SV40 gene. *J. Urol.*, **146**, 881–886.
35. Hayward, S.W. *et al.* (1995) Establishment and characterization of an immortalized but non-transformed human prostate epithelial cell line: BPH-1. *In Vitro Cell. Dev. Biol. Anim.*, **31**, 14–24.
36. Bello, D. *et al.* (1997) Androgen responsive adult human prostatic epithelial cell lines immortalized by human papillomavirus 18. *Carcinogenesis*, **18**, 1215–1223.
37. Thompson, E.W. *et al.* (2005) Carcinoma invasion and metastasis: a role for epithelial-mesenchymal transition? *Cancer Res.*, **65**, 5991–5995.
38. Veveris-Lowe, T.L. *et al.* (2005) Kallikrein 4 (hK4) and prostate-specific antigen (PSA) are associated with the loss of E-cadherin and an epithelial-mesenchymal transition (EMT)-like effect in prostate cancer cells. *Endocr. Relat. Cancer*, **12**, 631–643.
39. Tan, C. *et al.* (2001) Inhibition of integrin linked kinase (ILK) suppresses beta-catenin-Lef/Tcf-dependent transcription and expression of the E-cadherin repressor, snail, in APC-/- human colon carcinoma cells. *Oncogene*, **20**, 133–140.
40. Rosanò, L. *et al.* (2005) Endothelin-1 promotes epithelial-to-mesenchymal transition in human ovarian cancer cells. *Cancer Res.*, **65**, 11649–11657.
41. Medici, D. *et al.* (2010) Type I collagen promotes epithelial-mesenchymal transition through ILK-dependent activation of NF-kappaB and LEF-1. *Matrix Biol.*, **29**, 161–165.
42. Graff, J.R. *et al.* (2001) Integrin-linked kinase expression increases with prostate tumor grade. *Clin. Cancer Res.*, **7**, 1987–1991.
43. Heebøll, S. *et al.* (2009) Snail1 is over-expressed in prostate cancer. *APMIS*, **117**, 196–204.
44. Li, Y. *et al.* (2009) LEF1 in androgen-independent prostate cancer: regulation of androgen receptor expression, prostate cancer growth, and invasion. *Cancer Res.*, **69**, 3332–3338.
45. Troussard, A.A. *et al.* (2006) Preferential dependence of breast cancer cells versus normal cells on integrin-linked kinase for protein kinase B/Akt activation and cell survival. *Cancer Res.*, **66**, 393–403.
46. Younes, M.N. *et al.* (2005) Integrin-linked kinase is a potential therapeutic target for anaplastic thyroid cancer. *Mol. Cancer Ther.*, **4**, 1146–1156.
47. Attwell, S. *et al.* (2000) The integrin-linked kinase (ILK) suppresses anoikis. *Oncogene*, **19**, 3811–3815.
48. Hannigan, G.E. *et al.* (1996) Regulation of cell adhesion and anchorage-dependent growth by a new beta 1-integrin-linked protein kinase. *Nature*, **379**, 91–96.
49. Frisch, S.M. *et al.* (1994) Disruption of epithelial cell-matrix interactions induces apoptosis. *J. Cell Biol.*, **124**, 619–626.
50. Kang, Y.S. *et al.* (2010) Inhibition of integrin-linked kinase blocks podocyte epithelial-mesenchymal transition and ameliorates proteinuria. *Kidney Int.*, **78**, 363–373.
51. Demichelis, F. *et al.* (2007) TMPRSS2:ERG gene fusion associated with lethal prostate cancer in a watchful waiting cohort. *Oncogene*, **26**, 4596–4599.
52. McLaughlin, F. *et al.* (2001) Combined genomic and antisense analysis reveals that the transcription factor Erg is implicated in endothelial cell differentiation. *Blood*, **98**, 3332–3339.
53. Mehra, R. *et al.* (2008) Characterization of TMPRSS2-ETS gene aberrations in androgen-independent metastatic prostate cancer. *Cancer Res.*, **68**, 3584–3590.
54. Fuchs, B.C. *et al.* (2008) Epithelial-to-mesenchymal transition and integrin-linked kinase mediate sensitivity to epidermal growth factor receptor inhibition in human hepatoma cells. *Cancer Res.*, **68**, 2391–2399.
55. King, J.C. *et al.* (2009) Cooperativity of TMPRSS2-ERG with PI3-kinase pathway activation in prostate oncogenesis. *Nat. Genet.*, **41**, 524–526.
56. Persad, S. *et al.* (2000) Inhibition of integrin-linked kinase (ILK) suppresses activation of protein kinase B/Akt and induces cell cycle arrest and apoptosis of PTEN-mutant prostate cancer cells. *Proc. Natl. Acad. Sci. U.S.A.*, **97**, 3207–3212.
57. Edwards, L.A. *et al.* (2005) Inhibition of ILK in PTEN-mutant human glioblastomas inhibits PKB/Akt activation, induces apoptosis, and delays tumor growth. *Oncogene*, **24**, 3596–3605.

Received January 16, 2012; revised August 17, 2012; accepted September 8, 2012